

1 **PLASTIC WASTE GASIFICATION USING OXYGEN-ENRICHED AIR AND**
2 **STEAM: EXPERIMENTAL AND MODEL RESULTS FROM A LARGE**
3 **PILOT-SCALE REACTOR**

4 Francesco Parrillo¹, Filomena Ardolino¹, Gabriele Cali², Alberto Pettinai², Massimiliano
5 Materazzi³, Alex Sebastiani^{3*}, Umberto Arena¹

6 *¹ Department of Environmental, Biological, Pharmaceutical Sciences and Technologies – University of
7 Campania “Luigi Vanvitelli”, Via Vivaldi, 43, 81100 Caserta, Italy*

8 *² Sotacarbo S.p.A., Grande Miniera di Serbariu, 09013, Carbonia, CI, Italy*

9 *³ Department of Chemical Engineering, University College London, Torrington Place, London WC1E
10 7JE, United Kingdom.*

11
12
13 * *Author to whom correspondence should be addressed: a.sebastiani@ucl.ac.uk*
14

15 **ABSTRACT**

16 Advanced thermochemical technologies for plastic waste valorization represent an interesting
17 alternative to waste-to-energy options. They are particularly appealing for waste-to-hydrogen and
18 waste-to-chemicals applications, with autothermal steam-oxygen gasification in fluidized bed reactors
19 showing the greatest market potential. The study describes a series of experimental tests carried out
20 on a large pilot-scale fluidized bed gasifier, using steam and O₂-enriched air, with increasing fractions
21 of oxygen. Different values of the main operating parameters are varied: equivalence ratio (0.22-0.25),
22 steam-to-carbon ratio (0.7-1.13), and steam-to-oxygen ratio (up to 3.2). The fuel consists of real mixed
23 plastic waste coming from separate collection of municipal solid wastes. The data obtained are used
24 to investigate in depth the role of the main operating parameters and to improve and validate a
25 recently developed one-dimensional kinetic model for waste gasification. The validation shows a good

26 agreement between experimental data and model results, suggesting the reliability of the model to
27 predict the reactor behaviour under conditions of pure steam-oxygen gasification, relevant to many
28 industrial applications. It has been found that the equivalence ratio is the parameter that more affects
29 the syngas composition. At a constant equivalent ratio, the molar fraction of oxygen in the enriched
30 air shows a limited influence on syngas composition while the steam is crucial in controlling the
31 temperature along the reactor. Provided that the steam-to-carbon molar ratio is larger than 1.5, steam
32 affects mainly the reactor temperature rather than the syngas composition, qualifying the steam-to-
33 oxygen molar ratio as an instrumental parameter for smooth plant operation.

34

35 **KEYWORDS**

36 Plastic waste, Chemical recycling, Thermochemical conversion, Gasification, Pilot plant, Fluidized bed

LIST OF ACRONYMS	
BFBG	Bubbling Fluidized Bed Gasifier
CCE	Carbon Conversion Efficiency
CCS	Carbon Capture Storage
CGE	Cold Gas Efficiency
ER	Equivalence Ratio
GC	Gas-chromatograph
LHV	Low heating value
MPW	Mixed Plastic Waste
RDF	Refuse Derived Fuel
SNG	Synthetic Natural Gas
StC	Steam-to-Carbon molar ratio
StO ₂	Steam-to-Oxygen molar ratio
x _{O₂}	Oxygen molar fraction in the gasifying medium
XRF	X-ray fluorescence
WtCh	Waste-to-Chemicals
WtH ₂	Waste-to-Hydrogen

LIST OF SYMBOLS	
Q _{air}	Air flow rate injected into the gasifier
Q _{O₂ in air}	Oxygen flow rate inside the air input stream
Q _{N₂}	Nitrogen flow rate inside the air input stream
Q _{H₂O}	Steam flow rate injected into the gasifier
Q _{pure O₂}	Pure oxygen flow rate injected into the gasifier
Q _{O₂ total}	Total oxygen flow rate injected into the gasifier

Q_{fuel}	Fuel flow rate fed into the gasifier
------------	--------------------------------------

37

38 1. INTRODUCTION

39 1.1 Opportunities and challenges of thermochemical treatments of plastic waste by gasification.

40 Advanced thermochemical technologies, and gasification in particular, can be the efficient and
41 sustainable answer to the complex problem of mixed plastic waste (MPW) management (Suschem,

42 2020; Closed Loop Partners, 2022). This is supported by some important motivations. Gasification is a

43 well-recognized pathway to convert non-recyclable and unsorted MPW to fuels and valuable

44 chemicals (Hofbauer and Materazzi, 2019). Furthermore, it is also very flexible in terms of feedstock

45 uptake, so that it can be considered a “feedstock-agnostic” process (Afzal et al., 2023) able to convert

46 all C–C and C–O backbone polymers to mainly CO and H₂, due to the combined action of the high

47 temperature and selected oxidant (oxygen and/or steam). At the same time, the produced syngas - a

48 mixture of CO, H₂, CO₂, CH₄, and other light hydrocarbons - contributes to addressing the increasing

49 scale of MPW management and reducing the reliance on fossil fuels, like natural gas, for syngas

50 production at industrial scale. However, several areas of insufficient knowledge still exist, mainly

51 related to: the unique properties of plastic materials (e.g., melting behaviour and molecular weight

52 distribution) and intrinsic feedstock complexity (mixed polymers with different additives and

53 contaminants) (Madanikashani et al., 2022); the multi-scale nature of the process (high release of

54 volatiles that can affect reactor fluid dynamic, intricate reaction mechanisms and complex transport

55 phenomena in a multi-phase flow system) (Dogu et al., 2021); the severe cleaning standards required

56 for syngas utilisation (to make it suitable for efficient energy conversion systems or chemical syntheses

57 of high-added value products) (Boccia et al., 2021); the scale-up implications (complicated by the lack

58 of data from sufficiently large-scale reactors) (AECOM&FCE, 2021). Recent studies (Afzal et al., 2023;

59 Arena et al., 2023; Materazzi et al., 2023; Tomic et al., 2024) examined in detail the techno-economic
60 and sustainability potentials of plastic waste gasification, highlighting the great potential when
61 employing fluidized bed reactors for waste-to-hydrogen (WtH₂) and waste-to-chemicals (WtCh). In
62 both these promising fields, autothermal gasification using steam and oxygen as fluidizing/gasifying
63 media appears to have the largest potential for faster and more convenient deployment. This is due
64 to the numerous advantages that a nitrogen-free syngas provides, including higher heating values,
65 smaller volumes and unit operations associated, easier gas product separation (e.g. H₂ or SNG) and
66 better integration with CCS plants (Materazzi et al., 2023). However, most of the industrial waste-
67 fuelled gasifiers were developed as air-blown rather than oxygen-blown, and only a very limited
68 experience exists in autothermal steam-oxygen operations, particularly on large (pilot and
69 demonstrative scale) plants, as confirmed by recent techno-economic analyses (Afzal et al., 2023;
70 Tomic et al., 2022; 2024). To date, tests of plastic waste gasification have only been performed at
71 relevant scale in air-blown reactors (Langner et al., 2023; Arena and Di Gregorio, 2014), or allothermal
72 systems in which steam is the main gasification agent (Vela et al., 2024; Forero-Franco et al., 2023).
73 Such pilot tests have identified the opportunity to gasify different polymers, such as cable plastics and
74 polyolefins to generate a syngas rich in hydrogen and other light hydrocarbons, including olefins and
75 aromatics important for manufacturing industry. On the other hand, operational experience in
76 autothermal reactors using pure oxygen as oxidising agent is still at an early stage.

77 *1.2 Scope of the paper and its novelty.* The aforementioned complexities and challenges indicate that
78 experimental studies on sufficiently large-scale gasifiers are imperative to properly understand the
79 process, especially when treating plastic waste, and utilizing steam and oxygen as gasifying agents. An
80 adequate combination of experimental work and validated numerical modelling can be a solution to
81 define optimal process configurations, predict reactor performances, and establish design and
82 operating criteria, without involving time-consuming and resource-intensive experimental tests.

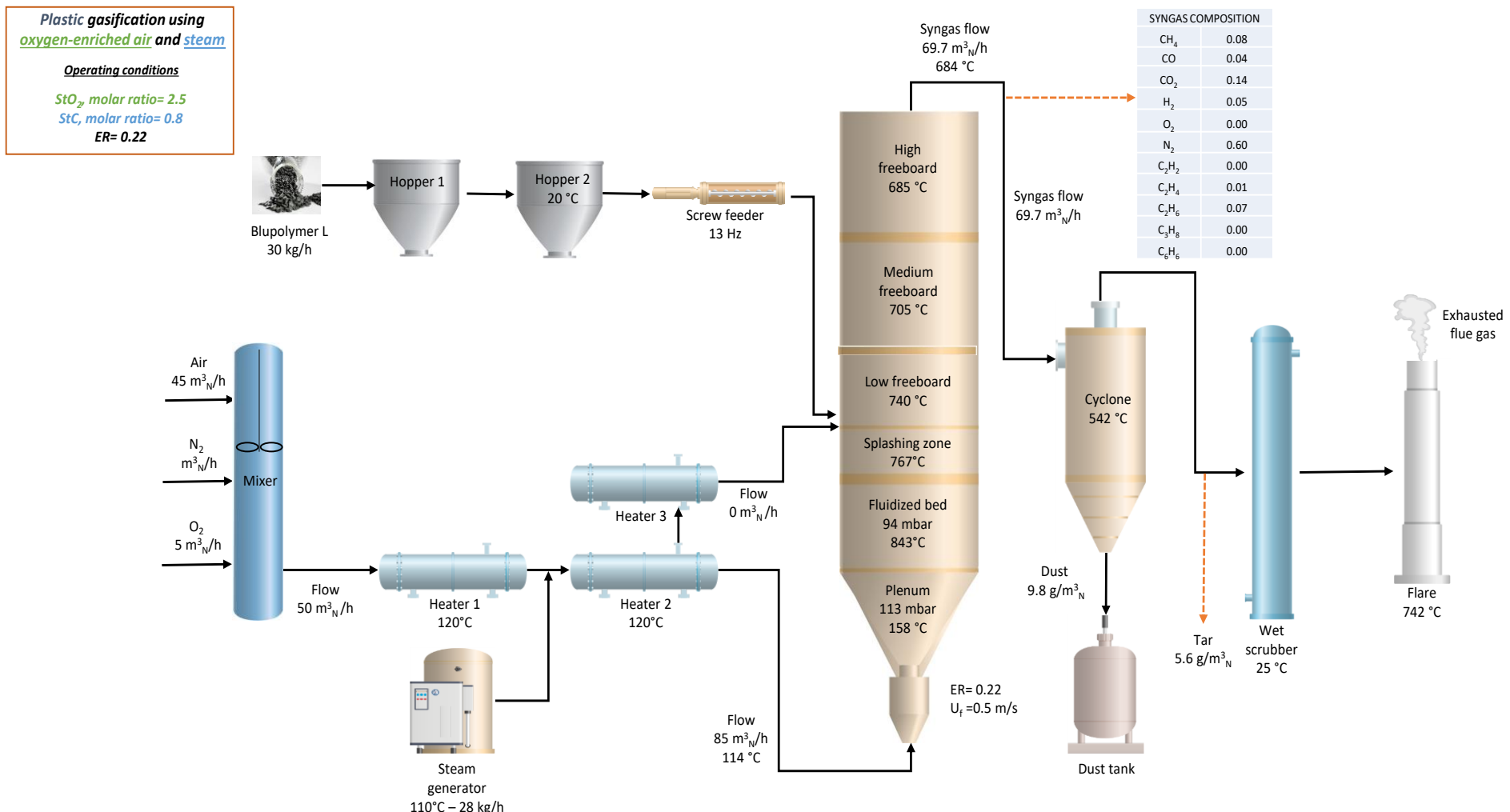
83 Despite this concept applies to any industrial process, it is particularly important for plastic waste
84 gasification, since the related numerical studies are either missing or oversimplified, as recently
85 highlighted by Dogu et al. (2021) and Madanikashani et al. (2022). Taking into account these
86 considerations, the study described here reports the experimental results obtained with a large pilot,
87 bubbling fluidized bed gasifier (BFBG) (Parrillo et al., 2021), operated with mixtures of steam and
88 oxygen-enriched air, at increasing O₂ molar fraction. The results were also used to inform, improve,
89 and validate a recently developed one-dimensional kinetic model for steam-oxygen gasification in
90 bubbling fluidized beds (Sebastiani et al., 2021). The so-validated model was then utilized to predict
91 the effects that new, and not yet investigated operating conditions of steam-oxygen gasification, can
92 have on the performance of a large-scale gasifier. This should simplify, make it cheaper, and drive the
93 design of new and dedicated experimental campaigns on large-scale facilities. To the best of authors'
94 knowledge, there are no papers in the scientific literature that refer to plastic gasification carried out
95 in a pilot-scale reactor, large enough to exclude any scale-related effect and operated with steam and
96 oxygen. All these aspects contribute qualifying the novelty of this work, which could benefit industrial
97 operators and new gasification plant developers in the plastic waste management sector.

98

99 **2. MATERIALS AND METHODS**

100 *2.1 The pilot scale gasifier.* The pilot scale bubbling fluidized bed gasifier employed in this study has a
101 maximum thermal input of 400 kW, with a plastic waste capacity up to 50 kg/h, and a reactor total
102 height (5.73 m) and internal diameter (0.489 m) that are large enough to exclude any scale-related
103 implications (Knowlton, 2013). This allows transferring obtained results to larger (even commercial)
104 scale reactors, and it contributes to bridging the gaps between research and industrial deployment.
105 Additional information regarding the main geometric parameters and features of the pilot scale BFBG
106 can be found in the ANNEX A, available in the Supplementary Material. The gasifier zones are

107 schematically shown in Figure 1: the plenum, the bed zone (up to 1.0 m), the splashing zone (up to
108 about 1.5 m), and the low (up to 2.45 m), medium (up to 3.45 m), and high freeboard (up to 5.7 m). K-
109 type thermocouples and pressure transmitters (Kobold) monitor the temperature and pressure of
110 each zone, which are continuously recorded and processed by a data acquisition and control system.
111 The raw syngas is cleaned by a cyclone and a wet scrubber to make it suitable for different final
112 applications. More details about the pilot scale gasifier can be found in Parrillo et al. (2021; 2023).
113 *2.2 The experimental procedure.* The gasifier requires about 3 hours to be heated up to about 700 °C
114 by means of pre-heated blast gases and three electric heaters located along the reactor. At this
115 temperature, the fluidizing gas and the plastic waste flow rates are set to obtain the desired values of
116 the process parameters. The mass flow rate of fluidizing gas (a mixture of air, oxygen, and steam) is
117 measured by means of a Bronkhorst, MF-C40 mass flow meter. Under the selected operating
118 conditions, and without any thermal assistance of external heaters, the reactor gradually reaches
119 thermal and chemical steady states, which are generally maintained for about 2 hours. During this
120 time, gas and solids sampling procedures are activated and measurements of pressure, temperature,
121 blast flow rates, and syngas composition (at four points: two levels along the reactor, at the reactor
122 exit, and downstream of the wet scrubber) are taken. The reliability of syngas composition
123 measurements is guaranteed by a double system of on-line monitoring downstream of the cleaning
124 section: a series of Siemens analysers to detect CO, CO₂, O₂ and CH₄ (Ultramat 23) and H₂ (Calomat 6);
125 and an Agilent 3000 gas-chromatograph (GC) equipped with 4 different columns (MolSieve, PoraPlot,
126 OV, Alumina) for the detection of a wide spectrum of syngas compounds. Gas is also sampled at two
127 points within the reactor (2450 mm and 3450 mm from the bottom) and at the reactor exit using
128 Tedlar bags and sent to off-line measurements, which are performed using the same GC mentioned
129 above. As reported in previous studies (Parrillo et al., 2021; 2023), tar content and composition were
130 measured by means of two methods. Tar concentration in the syngas is estimated conservatively by



131

132

Figure 1. Schematic flow sheet of the pilot scale bubbling fluidized bed apparatus, with data related to a typical run, carried out at equivalence ratio $ER=0.22$, steam/carbon ratio $StC=0.77$, steam/oxygen ratio $StO_2=2.45$, and fluidization velocity $U=0.5 \text{ m/s}$ (Dashed lines refer to sampling points).

134 imputing to the tar amount the whole carbon loading that, based on mass balances on atomic
135 species, cannot be attributed to either the produced gas or to the solids collected at the cyclone or
136 present inside the bed. Furthermore, a specific procedure is used to identify tar compounds
137 belonging to the classes between 2 and 5 of the classification proposed by Neeft et al. (2001); the
138 condensable species are sampled through six impinger bottles in-series, a suction pump, and a flow
139 meter operated with a known volumetric flow rate of syngas for about 30 min. The impinger bottles,
140 containing approximately 50 ml of isopropanol, are immersed in an ice bath at a temperature range
141 of -15°C/-20°C. The condensed hydrocarbons are off-line analysed with a specific pre-treatment in
142 a Perkin Elmer Clarus 500 gas chromatograph coupled with a mass spectrometer. Mass balances on
143 atomic species and the related energy balance for each test are performed by utilising data obtained
144 from on-line and off-line gas measurements and from chemical (proximate and ultimate) analyses
145 of collected elutriated fines. The flow rate of the produced syngas is determined using the tie-
146 component method (Felder et al., 2015) applied to the value of nitrogen content in the dry syngas,
147 as obtained by on-line and off-line GC measurements.

148 *2.3 The plastic waste and the bed material.* The plastic waste is a polyolefin blend, named
149 Blupolymer, provided by Corepla (Italian Consortium for Plastic Packaging), and prepared by the
150 I.Blu company (I.Blu, 2022) from non-recyclable residues of separated collection of plastics
151 packaging. Table 1 reports its ultimate analysis (obtained via a LECO Truspec CHN/S), together with
152 low heating value (LHV) and composition of the inorganic fraction. The bed material is made of
153 Austrian olivine particles, having a size range of 200-400 μm , with a Sauter mean diameter of 316
154 μm , a particle density of 2900 kg/m^3 and a bulk density of 1600 kg/m^3 . Olivine is a neo-silicate of
155 Mg and Fe, which can be represented by the formula $(\text{Mg},\text{Fe})_2\text{SiO}_4$. More information can be found

156 in Table A.1 of the ANNEX A in the Supplementary Material.

157 Table 1. Plastic waste characterisation of the plastic waste granules (Blupolymer)

<i>Ultimate analysis^a, %wt</i>	
C	83.7
H	12.4
N	0.2
O (by difference)	1.4
Moisture	0.01
Ash	2.4
<i>Heating Value, MJ/kg_{fuel}</i>	
LHV	40.5
<i>Ash composition (XRF analysis)^b, mg/kg</i>	
Al (as Al ₂ O ₃)	280
Ca (as CaO)	4200
Ba (as BaO)	-
Cr (as Cr)	-
Fe (as Fe ₂ O ₃)	180
P (as P ₂ O ₅)	-
Mg (as MgO)	<1000
Mn (as MnO)	-
Ni (as Ni)	10
K (as K ₂ O)	130
Si (as SiO ₂)	110
Ti (as TiO ₂)	-
S (as SO ₃)	-
Cl (as Cl ⁻)	.

^aAccording to the ASTM D 5373–02 and ASTM D 4239-05 standards

^bAccording to the standards EPA 051A2007 + EPA3010D2014 for the plastics waste

158

159 Olivine has a good catalytic activity that enhances the tar cracking reactions (Devi et al., 2003;
160 Mastellone and Arena, 2008); it is low cost and largely available in different parts of the world, and
161 shows high resistance to attrition phenomena, which is crucial for a bubbling fluidized bed
162 gasification process (Scala et al., 2013). The catalytic activity is enhanced by pre-calcination of the

163 bed particles at 900 °C for some hours, as suggested by Devi et al. (2003).

164 *2.4 The bubbling fluidized bed gasification model.* The experimental results obtained with the
165 described pilot scale BFBG are used to refine and validate a one-dimensional kinetic model for waste
166 gasification, developed on Matlab. The model is based on chemical reaction kinetics, coupled with
167 the typical features of a bubbling fluidized bed (Sebastiani et al., 2021). In particular, the fluidized
168 bed zone is modelled following the two-phase theory to describe the bed hydrodynamics,
169 specifically modified to capture the devolatilization behaviour of plastic feedstock (fed from above
170 the bed). The splashing zone is modelled following the ghost-bubble theory to consider the complex
171 mixing of the gas phases exiting the bed (Solimene et al., 2004), whilst the freeboard zone is
172 modelled as a non-isothermal plug flow reactor. The model incorporates the reaction network of
173 steam-oxygen gasification within the fluid dynamics of a fluidized bed to predict waste and tars
174 conversion, gas composition and overall gasification performance. The height of the bed is divided
175 into a series of compartments of suitable finite volume where the set of differential equations of
176 mass and energy balances are solved. The discretisation of the solutions could affect the accuracy
177 of the model; therefore, the grid size is chosen as an optimized compromise between precision and
178 computational time. Mass and energy balances are solved in each compartment, whereas the
179 output solution is used as input for the subsequent one. As the original model was developed for
180 RDF gasification, primary decomposition and secondary chemical reactions were further refined to
181 include mixed-plastic feedstock behaviour. In particular, the product distribution of primary
182 decomposition reactions, including pyrolysis of different plastic polymers, was defined according to
183 extensive data from similar-scale plant operations (Kaminsky, 2021; Iannello et al., 2023).
184 Subsequent conversion reactions, including oxidation, cracking, and reforming of the volatile

185 components were extended to include typical plastic-derived species, such as light olefins. The
186 entire set of chemical reactions for the simulations presented in this work is provided in the ANNEX
187 B available as supplementary material.

188

189 **3. RESULTS AND DISCUSSION**

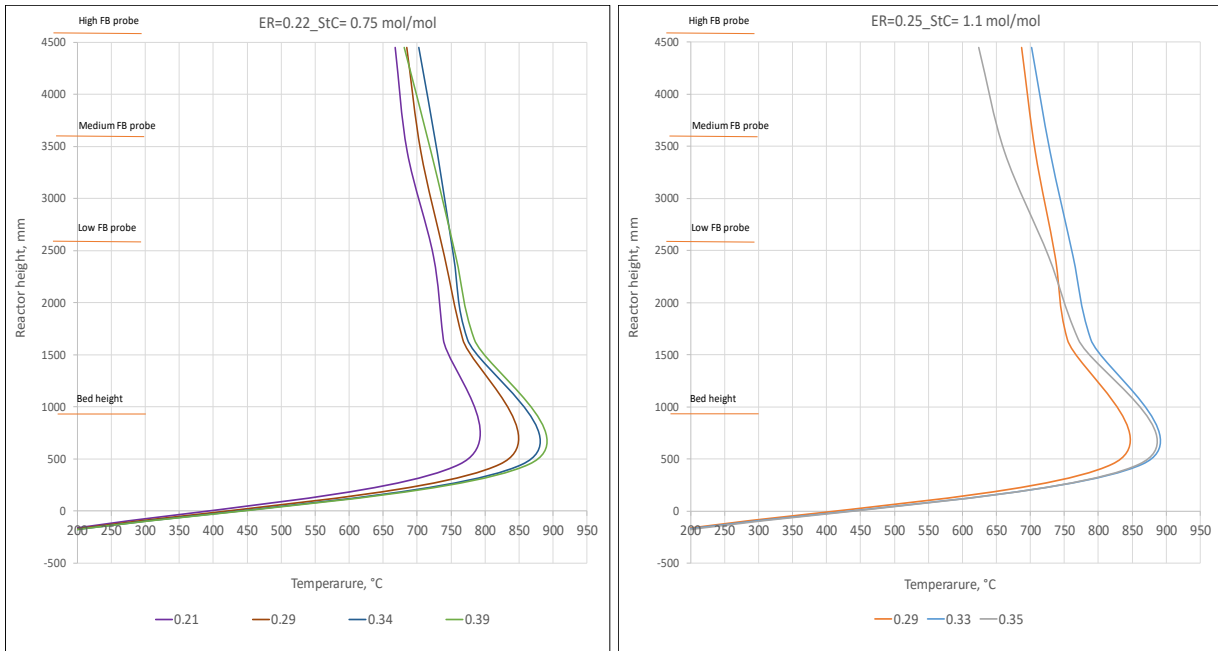
190 *3.1 The results of the experimental tests.* Autothermal gasification - whereby the energy required
191 for the endothermic reactions is provided by the partial oxidation of a limited amount of feedstock
192 - can be carried out with air, air and steam, or mixtures of air, steam, and pure oxygen. This requires
193 the monitoring and control of different operating and process performance parameters. Under
194 autothermal conditions, the temperature is a state variable of the system, therefore it is the result
195 of the reacting system to the imposed values of operating parameters (Arena, 2013). Nonetheless,
196 the temperature values are bounded within an admissible range, mainly related to the reactor
197 material strength (at the higher end) and the optimal progress of gasification reactions (at the lower
198 end). When air is the only gasifying (and fluidizing) agent, the unique and well-known operating
199 parameter is the equivalence ratio (ER), defined as the molar ratio between the oxygen fed to the
200 reactor and the amount required for stoichiometric combustion of fuel fed. ER is an essential
201 parameter that quantifies the oxygen needed to promote the necessary partial oxidation reactions.
202 Operating the gasifier with pure oxygen and steam as gasifying media has the main aim to reduce
203 or eliminate nitrogen gas, which would cause significant syngas dilution, undesired in WtH₂ or WtCh
204 applications (Hofbauer and Materazzi, 2019). In this case, the additional parameter steam-to-carbon
205 molar ratio (StC), defined as the ratio between the molar flowrate of steam and that of carbon

206 contained in the fed fuel, should be taken into account (Basu, 2010; Han et al., 2022). The
207 temperature of the reactor remains a state variable of the system, however, the role of thermal
208 moderator has to be performed by the steam, due to the reduced content or absence of nitrogen.
209 As a consequence, the inlet steam-to-oxygen molar ratio (StO_2) becomes an important parameter.
210 StO_2 is often associated to the moderator role served by the steam over partial combustion
211 reactions, affecting the selection of the StC , possibly resulting in values larger than those of interest
212 for thermodynamic reasons.

213 Table 2 reports the operating conditions of all the performed autothermal gasification tests, carried
214 out by treating about 30 kg/h of plastic waste. The first three experiments (test IDs A1-A3) utilize
215 only air as the gasifying agent to preliminary assess the reactor behaviour when operated with a
216 high heating value plastic waste and at different values of ER. The reactor temperature tends to
217 reach a thermal steady-state at high temperatures, close to the upper limit for safe operation of the
218 gasifier. The subsequent tests were then designed to investigate how the thermal steady-state and
219 BFBG performance are affected by a gradual modification of gasifying agents. In the first of these
220 tests (test ID AS1), steam was mixed with air, by keeping fixed ER at 0.22. As expected, steam worked
221 as a further temperature moderator (in addition to nitrogen), immediately reducing the bed
222 temperature from more than 900°C to 763°C. The following tests (test IDs ASO1-ASO9) utilised a
223 pure oxygen stream to gradually increase oxygen content in the gasifying medium (x_{O_2}), from 0.21
224 to 0.39. Two groups of tests were carried out at ER=0.22, with different StC (0.75 and 1.0), another
225 group utilised an ER=0.25, with $StC=1.1$.

Table 2. Operating conditions and main results of the pilot scale tests with the plastic waste.

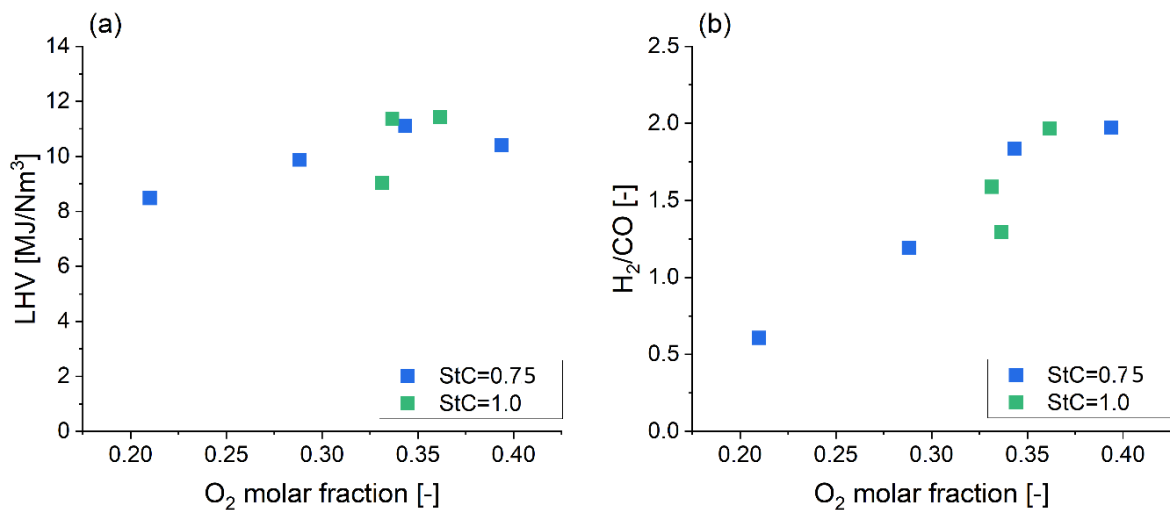
Operating and Process performance parameters		Test ID A1	Test ID A2	Test ID A3	Test ID AS1	Test ID ASO1	Test ID ASO2	Test ID ASO3	Test ID ASO4	Test ID ASO5	Test ID ASO6	Test ID ASO7	Test ID ASO8	Test ID ASO9
Gasifying medium														
Air	Q _{air} , L _N /h	112000	112000	66700	66800	44800	34200	30000	38100	37000	34000	42200	38200	33300
	Q _{air} , mol/h	4997	4997	2975	2980	2000	1500	1340	1700	1650	1510	1900	1700	1500
	Q _{O₂} in air, mol/h	1049	1049	625	630	420	320	280	360	350	320	400	360	310
	Q _{N₂} , mol/h	3948	3948	2350	2350	1580	1180	1060	1340	1300	1190	1500	1340	1190
Steam	Q _{H₂O} , L _N /h	0	0	0	36600	35200	35600	33100	43000	43400	44900	44300	44100	43500
	Q _{H₂O} , mol/h	0	0	0	1630	1570	1590	1480	1920	1940	2000	1980	1970	1940
Oxygen	Q _{pure O₂} , L _N /h	0	0	0	0	4900	7000	9100	6900	7100	8000	5000	6700	7100
	Q _{pure O₂} , mol/h	0	0	0	0	220	310	410	310	320	360	220	300	320
	Q _{O₂, total} , mol/h	1049	1049	625	630	640	630	690	670	670	670	620	660	630
Q _{fuel} , kg/h		53	46	29	29	28	31.7	31.7	30	30	29.5	26	27	25
Fluidization velocity, m/s		0.7	0.7	0.41	0.58	0.51	0.47	0.45	0.54	0.55	0.54	0.57	0.55	0.52
Equivalence ratio (ER), -		0.20	0.24	0.22	0.22	0.22	0.22	0.22	0.22	0.22	0.25	0.25	0.25	0.25
Steam/Carbon molar ratio (StC), -		0.00		0.75				1.0			1.1			
		(0)	(0)	(0)	(0.83)	(0.77)	(0.74)	(0.69)	(0.95)	(0.94)	(1.0)	(1.11)	(1.08)	(1.13)
O ₂ molar fraction (x _{O₂}), -		0.21	0.21	0.21	0.21	0.29	0.34	0.39	0.33	0.34	0.36	0.29	0.33	0.35
Steam/Oxygen molar ratio (StO ₂), -		0	0	0	2.61	2.45	2.52	2.15	2.89	2.87	2.97	3.20	3.00	3.10
Bed reactor temperature, °C		887	> 900	> 900	763	843	868	883	857	836	867	821	876	870
Syngas vol. flow rate, m ³ _N /h		146	137	88	87	70	61	59	64	64	63	63	68	58
Syngas LHV, kJ/m ³ _N		9380	6400	9221	8482	9882	11112	10405	9041	11362	11436	8799	10348	9566
Syngas specific energy, kWh/kg _{fuel}		7.1	5.3	7.75	7.1	6.4	5.92	5.36	5.40	6.66	6.83	5.91	7.22	6.06
Carbon conversion efficiency, -		0.76	0.65	0.78	0.74	0.69	0.63	0.61	0.63	0.72	0.73	0.68	0.79	0.71
Cold gas efficiency, -		0.67	0.50	0.72	0.66	0.63	0.55	0.50	0.50	0.62	0.63	0.55	0.67	0.56
H ₂ /CO		1.78	0.8	1.5	0.6	1.2	1.8	2.0	1.6	1.3	2.0	0.9	2.1	1.4
g _{H₂} /kg _{fuel}		14	15	12	10	11	12	13	13	11	14	9	17	11
g _{CO} /kg _{fuel}		109	211	111	221	130	87	93	111	116	101	133	113	112
Tar concentration, g/m ³ _N , syngas		28.8	3.4	3.4	3.4	5.6	8.6	6.5	9.6	11	8.6	4.5	10	7.4



228

229 Figure 2. Axial profiles of fluidized bed reactor temperature, as a function of oxygen content in the gasifying agent
 230 (xO_2), under different values of ER and StC.
 231

232 Figure 2 reports the measured temperature profiles along the reactor, where the average value in
 233 the bed reaches 883°C for an oxygen content of 39% at $StC=0.75$, and slightly lower at $StC=1.1$, with
 234 a limited reduction in the splashing zone. The profiles confirm the crucial role of nitrogen as
 235 temperature moderator. This role must be maintained when, under oxygen-steam operation,
 236 nitrogen is not part of the fluidization agent and must be replaced with a suitable amount of steam.
 237 Acceptable thermal steady states were reached only with $StO_2>2.5$. Figure 3 reports the values of
 238 some of the main process performance parameters as a function of increased oxygen content in the
 239 enriched-air stream and for different values of StC . It is difficult to isolate the effect of each gasifying
 240 agent as well as those of key operating parameters (ER and StC), as already observed in previous
 241 studies (Han et al., 2022).



242

243 Figure 3. Syngas low heating value (a) and H₂/CO ratio (b) as a function of the oxygen content in the enriched-air
244 stream, StC in the range 0.75-1.0 and constant ER at 0.22.

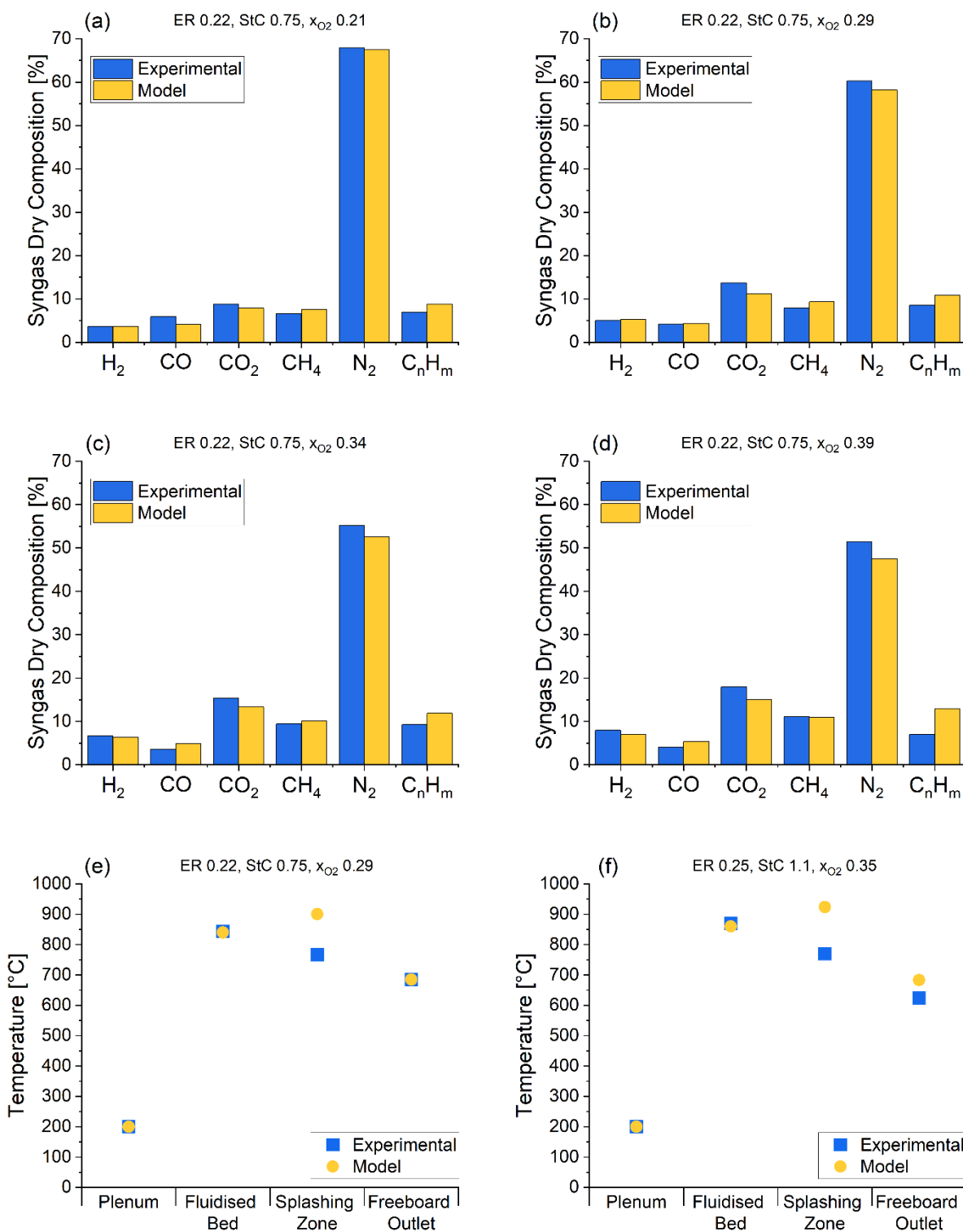
245

246 Oxygen-enriched air reduces the nitrogen dilution effect, thus increasing the syngas heating value
247 (Figure 3a). Notably, the obtained H₂/CO ratios (Figure 3b) are in the range of 1.5-2.5, which is of
248 particular interest for the synthesis of liquid fuels (Ciuta et al., 2018; Hofbauer and Materazzi, 2019).
249 Remarkable water content in the product syngas is also estimated (> 40%_{vol.}), indicating that a large
250 part of the steam is not utilised for conversion reactions. However, the role of steam as temperature
251 moderator remains crucial for system operation. Table 2, Figure 3 and Figures A.2 and A.3 in the
252 ANNEX A of the Supplementary Material, report all the obtained experimental data. Figure A.2
253 shows the values of Cold gas efficiency (CGE), Carbon conversion efficiency (CCE) and Syngas specific
254 energy, as a function of the oxygen content in the gasifying agent. Figure A.3 reports the feedstock
255 energy (i.e., the chemical energy of all compounds contained in each mass flow rate) at different
256 points of the experimental apparatus, under different operating conditions. At steady state, a
257 fraction of the energy entering the system with the plastic waste is lost in the gasifier to sustain the

258 operations and obtain the raw syngas, in agreement with the values of CGE reported in Figure A.2
259 (Arena and Di Gregorio, 2014).

260 *3.2 Comparison of the model with experimental results.* Figure 4 compares the syngas composition
261 and the reactor temperature profile at different conditions, as obtained by the experiments and
262 predicted by the model. The agreement is rather good, being the error in the range 1-5% for H₂
263 content, 1-10% for that of CO, and 6-10% for that of CH₄. This agreement is further supported by
264 the tables and figures reported in the ANNEX C, which detail the complete set of experimental and
265 modelling results. Nevertheless, an appreciable disagreement (in the order of 30%) is found for the
266 hydrocarbons content in the syngas, specifically the species C_nH_m with 2-4 carbon atoms. This could
267 be due to the limited availability of specific kinetic studies (and related equations) for C_nH_m in a
268 partially reducing atmosphere and to the assumed distribution of products released from the initial
269 devolatilisation stage, which is strongly dependent on the feedstock composition. This (partial) limit
270 of the model affects the accuracy of the predicted heating value of the obtained syngas.

271

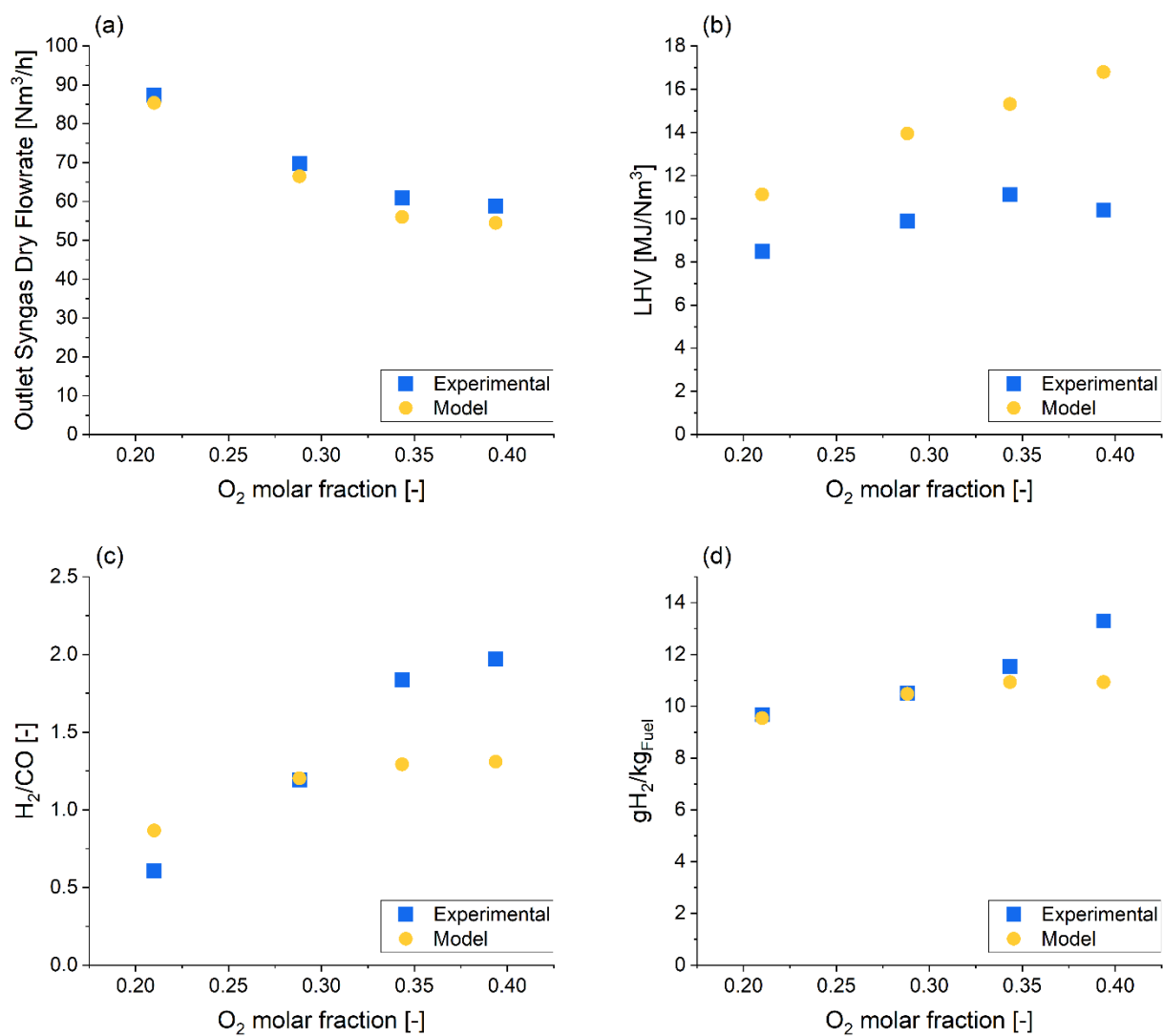


272

273
274

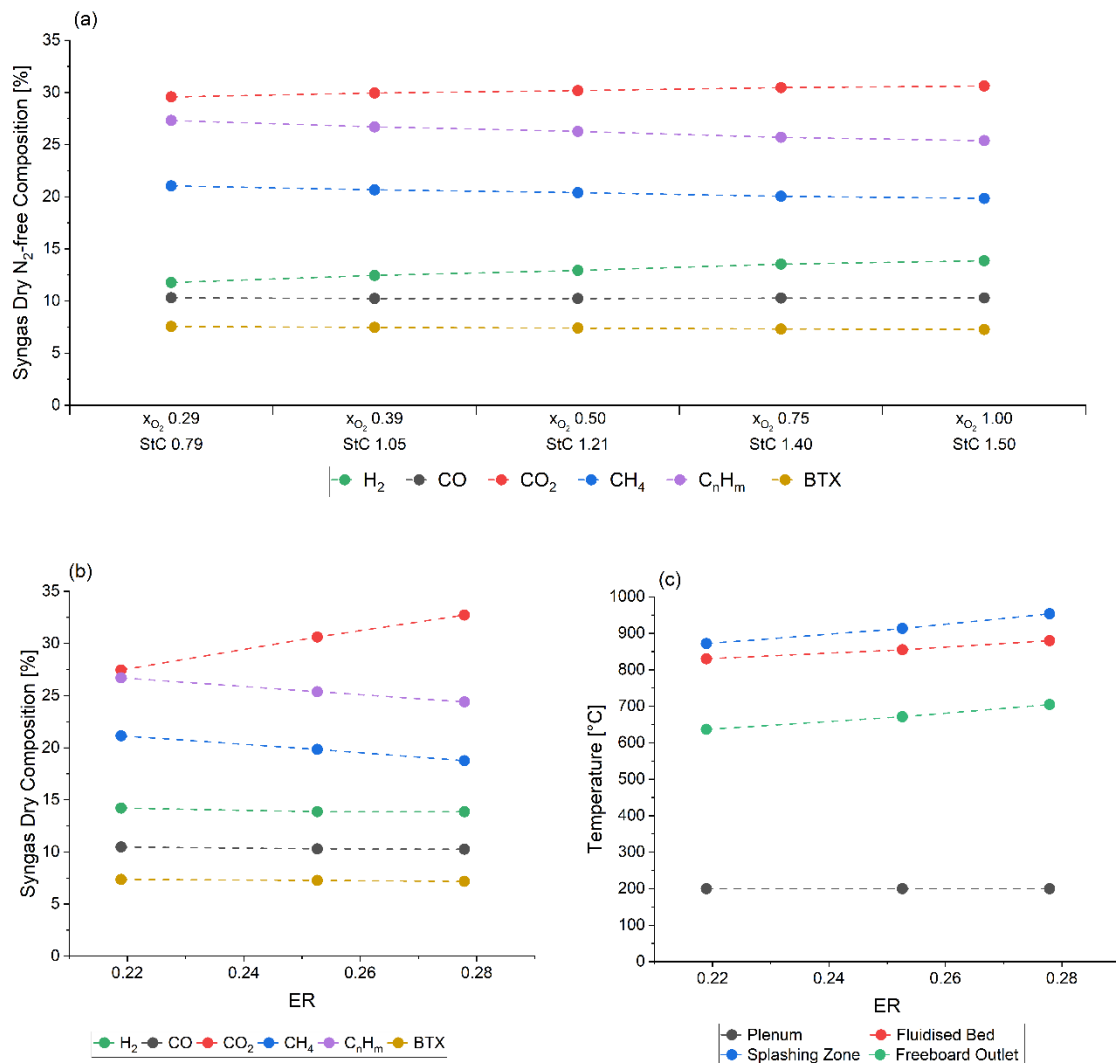
Figure 4 - Comparison between measured and predicted data of syngas dry composition (a to d) and reactor temperature profiles (e and f), at different operating conditions.

275 Figure 5 shows a fine agreement between experimental and model results for the volumetric syngas
 276 flow rate but clearly lower accordance in terms of syngas low heating values (i.e., predicted LHV)
 277 higher than the experimental values, due to the larger predicted values of C_nH_m content).
 278 Nonetheless, the trend is the same for increasing oxygen molar fraction in the gasifying medium.
 279 The rather good matching between results measured during the experimental tests on the large
 280 pilot scale gasifier and those obtained by the kinetic model suggests that the model could provide



281
 282 Figure 5 - Comparison between the experimental data and model results, as a function of x_{O_2} , ER 0.22, StC 0.75.

283 reliable information about the reactor behaviour also when the gasifier is operated with a mixture
284 of pure oxygen and steam. In particular, the model was interrogated to estimate the extent to which
285 StC (and, in turn, StO₂) must be increased to keep a constant bed temperature of 855°C in the
286 reactor, at ER=0.25, when the oxygen content in the enriched-air stream increases from 29% to
287 100%. The steam injection was increased progressively, from StC=0.79 at x_{O₂}=0.29 and StC=1.21 at
288 x_{O₂}=0.50, until StC=1.5 under conditions of pure oxygen-steam gasification. Figure 6a reports the
289 corresponding dry, and nitrogen-free syngas compositions, as predicted by the model. The results
290 indicate a limited increase in H₂ concentration (from 10.9% to 12.9%) and an even more limited
291 decrease in CH₄ (from 19.5% to 18.5%) and C_nH_m (from 28.1% to 26.3%). These variations appear in
292 agreement with the results provided by Erkiaga et al. (2013) and Li et al. (2021), obtained in a small-
293 scale apparatus. They could be explained by water-gas and steam reforming reactions, whose
294 extensions decrease when StC values are lower than the stoichiometric ones. Figure 6b reports
295 instead the variation of dry syngas composition, under conditions of pure oxygen-steam gasification,
296 at a fixed value of StC=1.5, as a function of ER. The latter appears the main parameter that affects
297 the syngas composition, resulting in an (expected) increase of carbon dioxide content (from 25.5%
298 to 30.5%), and a corresponding reduction of methane and C_nH_m (from 19.7% to 17.5%, and from
299 24.8% to 22.7%). Interestingly, StC seems to have a limited effect on syngas composition at values
300 larger than 1.5, possibly due to the limited residence time in the reactor for steam-reforming and
301 water-gas reactions to achieve equilibrium, as already suggested by Basu (2010). However, the role
302 of steam remains crucial to control the temperature profile of the reactor within an acceptable



303

304

305

306

307

308

309

310

311

Figure 6 – Model predictions at different conditions. Dry and N₂-free syngas composition (a) as a function of x_{O_2} and StC values able to keep the bed reactor temperature at 855°C with ER=0.25. Dry syngas composition (b) and temperature profile (c) as a function of ER, at pure oxygen-steam gasification conditions (StC=1.5).

312 under pure oxygen-steam conditions. When ER is increased, more heat is produced by partial
313 combustion reactions, resulting in an increase in temperature along the reactor.

314

315 **CONCLUSIONS**

316 This work investigates the autothermal plastic waste gasification process through pilot-scale
317 experiments carried out in a large bubbling fluidized bed reactor. The gasifier was operated with
318 steam and O₂-enriched air, at increasing fractions of oxygen, and with different values of
319 equivalence ratio, steam-to-carbon ratio, and steam-to-oxygen ratio. The results indicate that the
320 key process parameters are the equivalence ratio, which crucially affects the syngas composition,
321 and the steam-to-oxygen ratio, which allows for appropriate control of the reactor temperature
322 profile.

323 The obtained data were then used to validate a one-dimensional kinetic model for plastic waste
324 gasification, showing a rather good agreement between experimental and model data, with an error
325 in the range of 1-10% for the main syngas compounds, and a larger disagreement (in the order of
326 30%) only for the hydrocarbons with 2-4 carbon atoms.

327 The validated model has been used to predict the reactor behaviour under conditions of pure
328 oxygen and steam gasification. The results indicate a limited influence on the syngas composition of
329 the oxygen concentration in the fluidization/gasification agent. The steam can fulfil a pivotal role
330 both in the reactions and thermal stability of the process. However, provided that the steam-to-
331 carbon is larger than 1.5, the steam content affects mainly the reactor temperature control rather
332 than the syngas composition. These conclusions are extremely useful to industrial operators to

333 define optimal conditions for plant operations and comply with safety and performance targets.
334 The future research program will include further pilot-scale gasification tests carried out with larger
335 input flowrates of steam, while varying steam-to-oxygen ratio to control the temperature profile
336 along the fluidized bed reactor. These tests will be used to further improve the proposed model and
337 achieve better prediction of temperature profile and light hydrocarbons content in the syngas.

338

339 **SUPPLEMENTARY MATERIAL**

340 Additional data and information are available as Annexes associated with this article, in the online
341 version of the paper.

342

343 **ACKNOWLEDGEMENTS**

344 This work was carried out with the financial support of the Project 1.3 “Oxygen and Steam
345 Gasification of Plastics: Process design and techno-scientific support to the executive design of a
346 large-scale pilot plant” founded by The Italian Ministry of Environment and Energy Security in the
347 framework of the Research on Electric System programme, Research Plan 2022-2024.

348 The authors gratefully acknowledge the important contribution given by the consortium Corepla
349 and I.Blu company, providing the plastic waste from separate collection, utilised in all the
350 experimental tests.

351

352 **REFERENCES**

353 AECOM & Fichtner Consulting Engineers, 2021. Advanced Gasification Technologies – Review and
354 Benchmarking. Review of current status of advanced gasification technologies. Task 2 report for

355 Dept. for Business, Energy & Industrial Strategy.
356 <https://assets.publishing.service.gov.uk/media/615ec02be90e07197867ea85/agt-benchmarking-task-2-report.pdf>
357
358 Afzal, S., Singh, A., Nicholson, S.R., Uekert, T., DesVeaux, J.S., Tan, E.C.D., Dutta, A., Carpenter, A.C.,
359 Baldwin, R.M., Beckham, G.T., 2023. Techno-economic analysis and life cycle assessment of
360 mixed plastic waste gasification for production of methanol and hydrogen. Green Chem., 25,
361 5068. <https://doi.org/10.1039/d3gc00679d>
362 Arena, U., 2013. Fluidized bed gasification. In: Scala F, editor. Fluidized-bed technologies for near-
363 zero emission combustion and gasification. Woodhead, Publishing. ISBN 978-0-85709-541-1. p.
364 765-812. Chap. 17. <http://dx.doi.org/10.1016/B978-0-85709-541-1.50025-X>
365 Arena, U., Di Gregorio, F., 2014. Energy generation by air gasification of two industrial plastic wastes
366 in a pilot scale fluidized bed reactor. Energy, 68, 735-743.
367 <http://dx.doi.org/10.1016/j.energy.2014.01.084>
368 Arena, U., Parrillo, F., Ardolino, F., 2023. An LCA answer to the mixed plastics waste dilemma: Energy
369 recovery or chemical recycling? Waste Management, 171, 662-675.
370 [10.1016/j.wasman.2023.10.011](https://doi.org/10.1016/j.wasman.2023.10.011)
371 Basu, P, 2010. Biomass Gasification and Pyrolysis. Practical design and theory. p. 198. 1 Academic
372 Press-Elsevier, ISBN 978-0-12-374988-8
373 Boccia, C., Parrillo, F., Ruoppolo, G., Commodo, M., Berruti, F., Arena U., 2021. The Effect of Steam
374 Concentration on Hot Syngas Cleaning by Activated Carbons. Fuel Processing Technology, 204,
375 107033. <http://dx.doi.org/10.1016/j.fuproc.2021.107033>
376 Ciuta, S., Tsiamis, D., Castaldi, M.J., 2018. Field Scale Developments, Chap. 4 of Gasification of waste
377 materials (Editor(s): Simona Ciuta, Demetra Tsiamis, Marco J. Castaldi). Academic Press, ISBN
378 9780128127162, <https://doi.org/10.1016/B978-0-12-812716-2.00004-2>
379 Closed Loop Partners, 2022. Transitioning to a Circular System for Plastics. Assessing Molecular
380 Recycling_Technologies in the United States and Canada.
381 www.closedlooppartners.com/research/transitioning-to-a-circular-system-for-plastics-assessing-molecular-recycling-technologies-in-the-united-states-and-canada-2/
382
383 Devi, L., Ptasinski, K.J., Janssen, F.J.J.G., 2003. A review of the primary measures for tar elimination

384 in biomass gasification process. *Biom & Bioen*, 24, 125-140. [http://dx.doi.org/10.1016/S0961-9534\(02\)00102-2](http://dx.doi.org/10.1016/S0961-9534(02)00102-2)

385

386 Dogu, O., Pelucchi, M., Van de Vijver, R., Van Steenberge, P.H.M., D'hooge, D.R., Cuoci, A., Mehl, M.,
387 Frassoldati, A., Faravelli, T., Van Geem, K.M., 2021. The chemistry of chemical recycling of solid
388 plastic waste via pyrolysis and gasification: state-of-the-art, challenges, and future directions.
389 *Prog Energy Combust Sci*, 84, 100901. <https://doi.org/10.1016/j.pecs.2020.100901>

390 Erkiaga, A., Lopez, G., Amutio, M., Bilabao, J., Olazar, M., 2013. Syngas from steam gasification of
391 polyethylene in a conical spouted bed reactor. *Fuel*, 109, 461–469.
392 <http://dx.doi.org/10.1016/j.fuel.2013.03.022>

393 Felder, R.M., Rousseau, R.W., Bullard, L.G., 2015. Elementary principles of chemical processes. 4th
394 ed. J. Wiley & Sons. ISBN-13: 978-0-470-61629-1

395 Forero-Franco, R., Vela, I.C., Berdugo-Vilches, T., Gonzales-Aria, J., Maric., J. Thunman, H., Seemann,
396 M., 2023. Correlations between product distribution and feedstock composition in thermal
397 cracking processes for mixed plastic waste. *Fuel*, 341, 127660.
398 <https://doi.org/10.1016/j.fuel.2023.127660>

399 Han, S.W., Tokmurzin, D., Lee, J.J., Lee, S.H., Park, S.J. et al., 2022. Gasification characteristics of
400 waste plastics (SRF) in a bubbling fluidized bed: Use of activated carbon and olivine for tar
401 removal and the effect of steam/carbon ratio. *Fuel*, 314, 123102.
402 <https://doi.org/10.1016/j.fuel.2021.123102>

403 Hofbauer, H. and Materazzi, M., 2019. Waste gasification processes for SNG production. In:
404 Materazzi M, Foscolo PU, editors. Substitute natural gas from Waste. Technical assessment and
405 industrial applications of biochemical and thermochemical processes. Elsevier.105-60.
406 <http://dx.doi.org/10.1016/B978-0-12-815554-7.00007-6.>

407 Iannello, S., Bond, Z., Sebastiani, A., Errigo, M., Materazzi, M., 2023. Axial segregation behaviour of
408 a reacting biomass particle in fluidized bed reactors: experimental results and model validation.
409 *Fuel*. 338, 127234. <http://dx.doi.org/10.1016/j.fuel.2022.127234>

410 I.Blu, 2022. <https://www.iblu.it/en/products.html>

411 Knowlton, T., 2013. Fluidized bed reactor design and scale-up. In: Scala F, editor. Fluidized-bed
412 technologies for near-zero emission combustion and gasification. Woodhead, Publishing. ISBN

413 978-0-85709-541-1. p. 481-523. Chap. 10. <http://dx.doi.org/10.1016/B978-0-85709-541-1.1.50025-X>

414

415 Langner, E., Kaltenmorgen, Heinze, J.C., Ströhle, J., Epple, B., 2023. Fluidized bed gasification of solid
416 recovered fuels in a 500kWth pilot plant. Fuel, 344, 127901,
417 <https://doi.org/10.1016/j.fuel.2023.127901>

418 Li, S., Vela, I.C., Jarvinen, M., Seemann, M., 2021. Polyethylene terephthalate (PET) recycling via
419 steam gasification – The effect of operating conditions on gas and tar composition. Waste
420 Management. 130, 117-126. <http://dx.doi.org/10.1016/j.wasman.2021.05.023>

421 Madanikashani, S., Vandewalle, L.A., De Meester, S., De Wilde, J., Van Geem, K.M., 2022. MultiScale
422 Modeling of Plastic Waste Gasification: Opportunities and Challenges. Materials 2022, 15, 4215.
423 <http://dx.doi.org/10.3390/ma15124215>

424 Mastellone, M.L. and Arena, U., 2008. Olivine as tar removal/catalyst during the fluidized bed
425 gasification of a plastic waste. AIChE J, 54/6, 656-1667. <http://dx.doi.org/10.1002/aic.11497>

426 Materazzi, M., Chari, S., Sebastiani, A., Lettieri, P., Paulillo, A., 2023. Waste-to-energy and waste-to-
427 hydrogen with CCS: Methodological assessment of pathways to carbon-negative waste
428 treatment from an LCA perspective. Waste Management. 173, pp. 184-199.
429 <http://dx.doi.org/10.1016/j.wasman.2023.11.020>

430 Neeft, J.P.A., Knoef, H.A.M., Buffinga, G.J., Zielke, U., Sjöström, K., Brage, C., Hasler, P., Smell, P.A.,
431 Suomalainen, M., Dorrington, M.A., Greil ,C., 2001. Guideline for Sampling and Analysis of Tar
432 and Particles in Biomass Producer Gases. Version 3.3.
433 <http://dx.doi.org/10.1002/9780470694954.ch11>

434 Parrillo, F., Ardolino, F., Cali', G., Marotto, D., Pettinai, A., Arena, U., 2021. Fluidized bed gasification
435 of eucalyptus chips: axial syngas profiles in a pilot scale reactor. Energy, 219, 119604.
436 [http://dx.doi.org/10.1016/j.energy.2020.119604.](http://dx.doi.org/10.1016/j.energy.2020.119604)

437 Parrillo, F., Boccia, C., Ruoppolo, G., Commodo, M., Berruti, F., Arena, U. 2023. Steam reforming of
438 tar in hot syngas cleaning by different catalysts: removal efficiency and coke layer
439 characterization. The Canadian Journal of Chemical Engineering. 101, 97-109.
440 [https://doi.org/10.1002/cjce.24535.](https://doi.org/10.1002/cjce.24535)

441 Parrillo, F., Ardolino, F., Boccia, C., Calì, G., Marotto, D., Pettinai, A., Arena, U., 2023. Co-Gasification

442 of Plastics Waste and Biomass in a Pilot Scale Fluidized Bed Reactor, Energy, 273, 127220.
443 <http://dx.doi.org/10.1016/j.energy.2023.127220>

444 Scala, F., Chirone, R., Salatino, P., 2013. Attrition phenomena relevant to fluidized bed combustion
445 and gasification systems. In: Scala F, editor. Fluidized-bed technologies for near-zero emission
446 combustion and gasification. Woodhead, Publishing. ISBN 978-0-85709-541-1. p. 286-287. Chap.
447 6. <http://dx.doi.org/10.1016/B978-0-85709-541-1.50025-X>

448 Schwarz, A.E., Lensen, S.M.C., Langeveld, E., Parker, L.A., Urbanus, J.H., 2023. Plastics in the global
449 environment assessed through material flow analysis, degradation and environmental
450 transportation. SciTotEnv, 875, 162644. <http://dx.doi.org/10.1016/j.scitotenv.2023.162644>

451 Sebastiani, A., Macrì, D., Gallucci, K., Materazzi, M., 2021. Steam - oxygen gasification of refuse
452 derived fuel in fluidized beds: Modelling and pilot plant testing. Fuel Processing Technology. 216,
453 106783. <http://dx.doi.org/10.1016/j.fuproc.2021.106783>

454 Solimene, R., Marzocchella, A., Ragucci, R., Salatino, P. 2004. Flow Structures and Gas-Mixing
455 Induced by Bubble Bursting at the Surface of an Incipiently Gas-Fluidized Bed. Ind. Eng. Chem.
456 Res., 43, 18, 5738–5753. <https://doi.org/10.1021/ie049729x>

457 Suschem, 2020. Sustainable Plastics Strategy. Available at: <http://www.suschem.org/publications>.

458 Tomić, T., Slatina, I., Schneider, D.R., 2022. Thermochemical recovery from the sustainable economy
459 development point of view-LCA-based reasoning for EU legislation changes. Clean Technol
460 Environ Policy 24, 3093-3144. <https://doi.org/10.1007/s10098-022-02346>

461 Tomić, T., Slatina, I., Schneider, D.R., 2024. Techno-economic review of pyrolysis and gasification
462 plants for thermochemical recovery of plastic waste and economic viability assessment of
463 small-scale implementation. Clean Technologies and Environmental Policy, 26, 171-195.
464 <https://doi.org/10.1007/s10098-023-02648-3>

465 Vela, I.C., Maric, J., Gonzales-Aria, J., Seemann, M., 2024. Feedstock recycling of cable plastic residue
466 via steam cracking on an industrial-scale fluidized bed, Fuel, 355, 129518,
467 <https://doi.org/10.1016/j.fuel.2023.129518>